

NJC

Accepted Manuscript



This is an *Accepted Manuscript*, which has been through the Royal Society of Chemistry peer review process and has been accepted for publication.

Accepted Manuscripts are published online shortly after acceptance, before technical editing, formatting and proof reading. Using this free service, authors can make their results available to the community, in citable form, before we publish the edited article. We will replace this *Accepted Manuscript* with the edited and formatted *Advance Article* as soon as it is available.

You can find more information about *Accepted Manuscripts* in the [Information for Authors](#).

Please note that technical editing may introduce minor changes to the text and/or graphics, which may alter content. The journal's standard [Terms & Conditions](#) and the [Ethical guidelines](#) still apply. In no event shall the Royal Society of Chemistry be held responsible for any errors or omissions in this *Accepted Manuscript* or any consequences arising from the use of any information it contains.



www.rsc.org/njc



Pd-Grafted Functionalized Mesoporous MCM-41: A Novel, Green and Heterogeneous NanoCatalyst for the Selective Synthesis of Phenols and Anilines from Aryl Halides in Water

Forugh Havasi^a, Arash Ghorbani-Choghamarani^{b*} and Farzad Nikpour^a

Received 00th January 20xx,
Accepted 00th January 20xx

DOI: 10.1039/x0xx00000x

www.rsc.org/

A new type of mesoporous-recoverable catalyst was synthesized by the immobilization of Pd on the surface of functionalized mesoporous MCM-41 and used as an efficient, recoverable and thermally stable heterogeneous nano catalyst for the synthesis of phenols and anilines from aryl halides in water. Nanospherical MCM-41 silica with an average size of 40 nm and pore diameter of 3 nm was prepared through sol-gel procedure. The catalyst was characterized by FT-IR, XRD, SEM, TEM, TGA, EDS and ICP techniques. MCM-41-dtz-Pd showed excellent catalytic activity for the synthesis of phenols and anilines under mild reaction conditions. The heterogeneous catalyst showed good recyclability and can be reused many times without significant loss of its catalytic activity. Also, the EDS results show very low leaching of palladium during the catalytic process (about 1%).

1 Introduction

Over the past several decades “Green Chemistry” has demonstrated how fundamental scientific methodologies can protect human health and the environment in an economically beneficial manner. Significant progress is being made in several key research areas, such as catalysis, the design of safer chemicals and environmentally benign solvents [1]. The application of catalysts to reduced systems toxicity, benign and renewable energy systems and reaction efficiency, make them as a central focus area for green chemistry research [1, 2]. In the last few years, immobilization of homogeneous catalysts on various solid supports with the advantage of catalysts separation and recycling has been widely studied in many divergent areas of research [3, 4]. However, immobilization of homogeneous catalysts usually, decreases the catalytic activity [5, 6]. This drawback can be overcome using nanomaterials as ideal heterogeneous supports. Because nano-sized catalysts can serve as efficient bridge and fill the gap between homogeneous and heterogeneous catalysts [7]. Among different nanoparticles, mesoporous silica, especially MCM-41, is commonly employed as a heterogeneous support for the immobilization of homogeneous catalysts. MCM-41 has a hexagonal arrangement of one-dimensional mesopores with diameters ranging from 2 to 10 nm [8]. Due to its unique properties such as high surface area, homogeneity of the

pores, good thermal stability, tunable and accessible pores, MCM-41 has been a focus for several research areas like nanoscience [9], catalysis [10-12] environmental purification [13], absorption [14] and drug delivery [15]. The nature of MCM-41 pore structure can be used to functionalize *via* reaction with alkoxysilyl compounds and then, incorporation of metal complexes into the channel walls [16]. Stepnicka [17, 18] and Karimi [19] modified mesoporous silica with various *N*-groups and loaded this support with palladium. The resulting material was applied as a catalyst for organic synthesis. *O*-Arylation and *N*-arylation coupling reactions catalyzed by transition-metals are among the most important reactions in organic synthesis [20, 21]. Phenols and anilines are important building blocks for constructing natural products, pharmaceutical and medicinal compounds, as well as in polymers and materials [22, 23]. Thus, the development of highly efficient methods for the synthesis of these compounds under mild reaction conditions has gained considerable attention in synthetic chemistry. Also, the development of a cheaper system enabling the hydroxylation [24, 25] and amination [21, 26] of aryl halides has become an important goal. The transition-metal-catalyzed cross-coupling reaction of aryl halides with hydroxide salts and aqueous ammonia represents a direct, convenient, regioselective and relatively atom-economical process to afford phenols and anilines [27-29]. The Cu-catalyzed hydroxylation of aryl bromides and iodides has been applied to prepare a wide range of functionalized phenols [30, 31]. These Cu-catalyzed protocols are generally limited to the use of electron deficient aryl chlorides coupling partners [32-34], however, the analogous Pd-catalyzed process is complementary in this regard and potentially capable of transforming a broader

^a Department of Chemistry, Faculty of Sciences, University of Kurdistan, P.O. Box 66315-416, Sanandaj, Iran

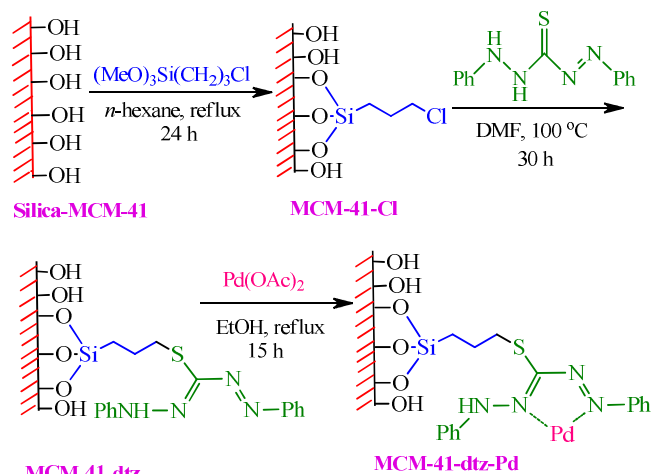
^b Address correspondence to A. Ghorbani-Choghamarani, Department of Chemistry, Faculty of Science, Ilam University, P.O. Box 69315516, Ilam, Iran; Tel/Fax: +98 841 2227022; E-mail address: arashghch58@yahoo.com or a.ghorbani@mail.ilam.ac.ir

scope of aryl halides to phenols and derivatives thereof [29, 35, 36]. Recently, several efficient palladium/phosphine-catalysed processes have been developed for selective formation of phenols [37] and anilines [38]. In general, the activity of homogeneous palladium catalysts such as Pd(OAc)₂ and PdCl₂ is sufficiently high, however, they suffer from the drawbacks of difficult separation and recovering from the reaction mixture as well as serious environmental pollution, which have limited their applications. Development of heterogeneous palladium catalysts to overcome the above drawbacks has important theoretical and practical significance and also is one of the main objectives of green chemistry. Thus, solid materials such as polymer materials, carbon, zeolite and different types of silica such as amorphous silica, mesoporous molecular sieves and solids obtained by co-condensation of silicate precursors have been used to immobilize the palladium catalysts [39-41].

In this paper, we report the synthesis and characterization of Pd complex supported on dithizone-functionalized nanostructured MCM-41 (MCM-41-dtz-Pd), which has been applied as a novel and efficient catalyst for the synthesis of phenols and anilines from aryl halides in water at room temperature.

2 Results and discussion

In continuation of our recent success in the introduction of new catalysts [42-44], herein we report the synthesis of Pd complex supported on dithizone-functionalized nanostructured MCM-41 (MCM-41-dtz-Pd) as a novel and efficient catalyst for the synthesis of phenols and anilines from aryl halides in water (Scheme 1).



Scheme 1. Preparation process of MCM-4-dtz-Pd

2.1 Catalyst characterization

Pd complexes supported on nanoporous MCM-41 have been characterized by FT-IR, TGA, XRD, SEM, TEM, EDS and ICP techniques and also by their comparisons with that of authentic samples [42-45].

Successful functionalization of the mesoporous MCM-41 can be inferred from FT-IR technique. FT-IR spectra were

recorded separately at different stages of the preparation (Fig. 1). Curve **a** in Fig. 1 is the spectrum of MCM-41 and curve **b** is the spectrum of MCM-41-*n*Pr-Cl. The absorption band presented at 960 cm⁻¹ is attributable to Si-O vibrations [46]. Absorption bands at 1228, 1077, 790 and 460 cm⁻¹ are assignable to the asymmetric and symmetric stretching vibrations of the mesoporous framework (Si-O-Si). The O-H stretching vibration bands appeared at 3460 cm⁻¹. The presence of the anchored CPTMS group is confirmed by C-H stretching vibrations at 2940 and 2847 cm⁻¹ in MCM-41-*n*Pr-Cl spectra. The curve **c** shows stretching vibrations at 1640 cm⁻¹ (C=N), 1425 cm⁻¹ (C=C) and broad band at 3440 cm⁻¹ (O-H and N-H) for MCM-41-dtz. Curve **d** shows the FT-IR spectrum after adsorption of Pd on to MCM-41-dtz.

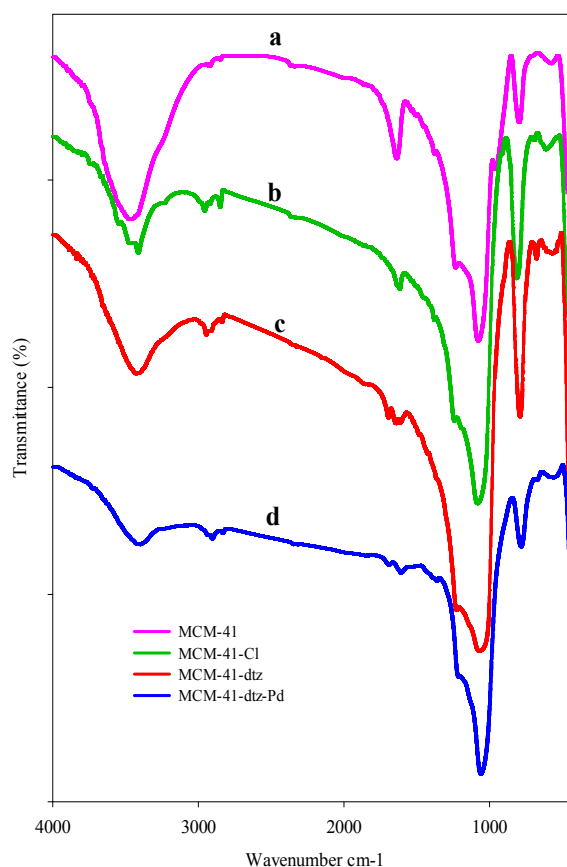


Figure 1. FT-IR spectra of (a) MCM-41 (b) MCM-41-*n*Pr-Cl, (c) MCM-41-dtz, (d) MCM-41-dtz-Pd

The X-ray diffraction patterns of MCM-41, MCM-41-*n*Pr-Cl, MCM-41-dtz and MCM-41-dtz-Pd are shown in Fig. 2. These spectra indicate that one-dimensional hexagonal mesoporous structure of MCM-41 was obtained. The MCM-41 pattern exhibits very sharp (100) diffraction peak at 2.46 2-theta and two additional high order peaks (110 and 200) with lower intensities at 4.17 and 4.68 2-theta, respectively [47]. The values of d-spacing (100) for XRD pattern of

MCM-41, MCM-41-*n*Pr-Cl, MCM-41-dtz and MCM-41-dtz-Pd were 38.10, 36.53, 35.79 and 35.40 Å, respectively. A unit cell parameter, a_0 was obtained using the following equation:

$$a_0 = \frac{2d_{100}}{\sqrt{3}}$$

All of the samples showed one intense peak (100) and the patterns were similar to that of pure silica MCM-41, indicating that the functionalized MCM-41 materials contain ordered hexagonal arrays of one-dimensional channel structure. After the functionalization steps, a considerable decrease in the XRD peaks intensity was observed. It should be noted that the intensity decrease in the (100) peak for functionalized MCM-41 providing further evidence of functionalization occurring mainly inside of mesopore channels [10]. This phenomenon indicates that MCM-41 structure unchanged and the Pd complex is well dispersed on the inner channel pores. Therefore, it can be concluded that the formation of the catalyst has taken place preferentially inside the pore system of MCM-41.

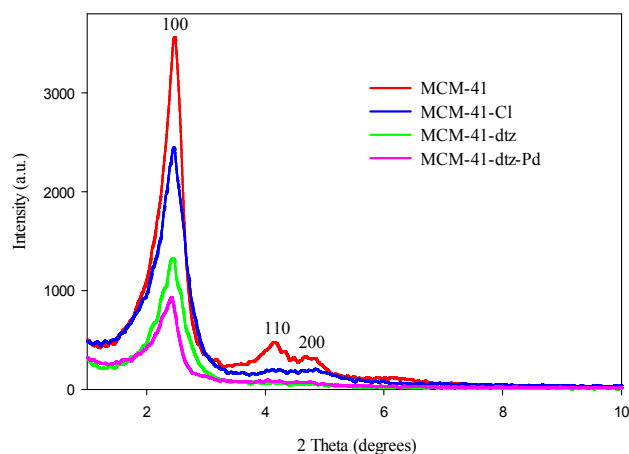


Figure 2. Low angle XRD patterns of MCM-41, MCM-41-*n*Pr-Cl, MCM-41-dtz and MCM-41-dtz-Pd.

Immobilization of Pd complexes on functionalized mesoporous MCM-41 can also be inferred from thermogravimetric analysis (TGA) diagram. The TGA was also used to determine the percentage of chemisorbed organic functional groups onto the MCM-41 mesoporous. The TGA curves of MCM-41, MCM-41-*n*Pr-Cl, MCM-41-dtz and MCM-41-dtz-Pd show the mass loss of the organic materials as they decompose upon heating (Fig. 3). According to these curves, two weight loss steps were observed. The first mass loss occurs at a temperature range of 25-300 °C that is related to the loss of physically and chemically adsorbed water and organic solvents. The second mass loss occurs at a temperature range of 300-780 °C, which is related to the thermal decomposition of organochloropropyl fragments and organic ligands in the complex.

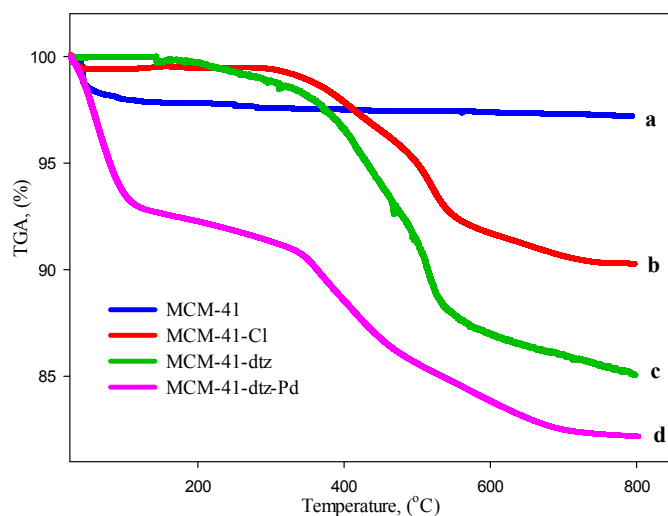


Figure 3. TGA curves of MCM-41 (a), MCM-41-*n*Pr-Cl (b), MCM-41-dtz (c) and MCM-41-dtz-Pd (d).

The energy dispersive spectrum (EDS) of described nanostructured MCM-41 showed that the relative mass percents of C, N, O, Si, S, and Pd are 11.06%, 1.79%, 23.29%, 22.57%, 2.27 and 39.03%, respectively. A typical EDS spectrum of MCM-41-dtz-Pd was shown in Fig. 4. The EDS spectrum at different points of the image confirms the presence of Pd in the mesoporous silica matrix. The amount of Pd incorporated into the mesoporous silica found to be 10%, which determined by inductively coupled plasma optical emission spectrometry (ICP-OES).

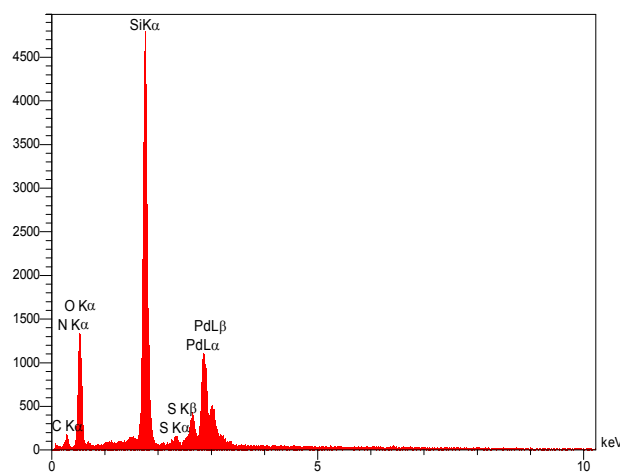


Figure 4. EDS pattern of MCM-41-dtz-Pd.

Morphological changes were investigated by scanning electron microscopy (SEM) of MCM-41 and MCM-41-dtz-Pd (Fig. 5a, 5b). Fig. 5c and Fig. 5d show transmission electron micrographs of representative regions of MCM-41. Highly ordered long-range hexagonal arrangement of the pores can be clearly observed. The TEM results are in good agreement with the XRD.

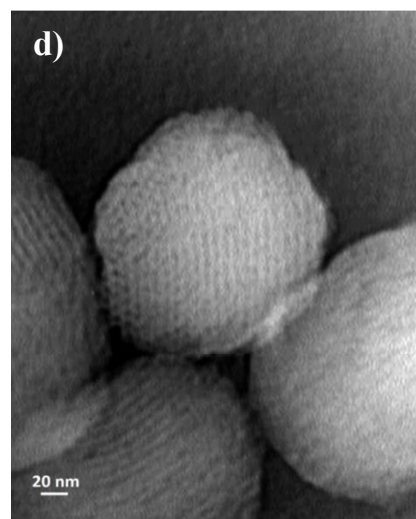
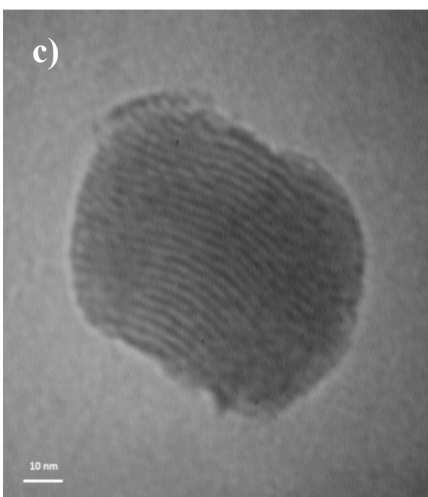
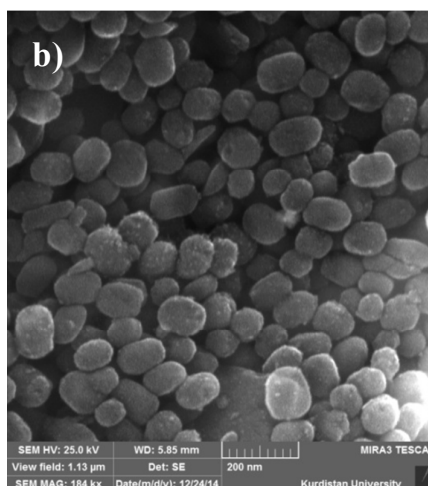
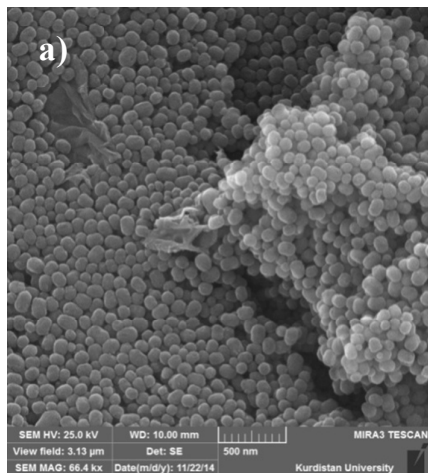
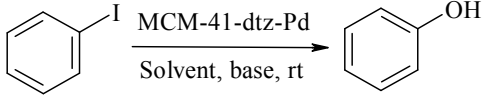


Figure 5. SEM image of calcined MCM-41/ MCM-41-dtz-Pd (a and b), TEM image of calcined MCM-41(c and d).

2.2 Catalytic studies

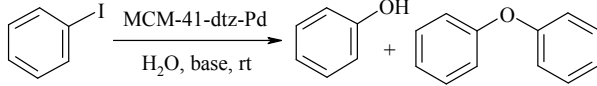
The activity of described catalyst was investigated through a reaction of aryl halides with KOH and $\text{NH}_3 \cdot \text{H}_2\text{O}$ for the synthesis of phenol and aniline derivatives. Initially, we examined the reaction of iodobenzene with KOH in different solvents, bases and various catalytic amounts of MCM-41-dtz-Pd (Table 1). Applying 7 mg of MCM-41-dtz-Pd and 2 mmol of KOH as base in 3 mL H_2O at room temperature, is the best conditions for the hydroxylation of iodobenzene (1.0 mmol) (Table 1, entry 4). Other bases such as NaOH, K_2CO_3 , K_3PO_4 and different solvents including DMF, DMSO and PEG were tested and outcome of the reactions were unsatisfactory. Also, the use of higher amount of catalyst (10 mg) does not effectively improve the yield of reaction (Table 1, entry 5). During the optimization of the reaction conditions for conversion of aryl halides to phenols, we observed that hydroxide bases provided optimal results. When 2.0 mmol of KOH was used, the phenol product predominates since attack on the MCM-41-dtz-PdAr(X) species by hydroxide occurs much faster than attack by in-situ generated KOAr. Of note, when 1.0 mmol KOH is used, the phenol is still the major product (Table 2). Interestingly, it was found that in the presence of other bases such as K_3PO_4 or K_2CO_3 , no phenol product was isolated, while conversion of the aryl halide to its symmetrical diaryl ether derivatives was observed. In this case, the rate of phenol formation must be less than the rate of diaryl ether formation (Table 2).

Table 1. Optimization of the hydroxylation of iodobenzene^a


Entry	Cat. (mg)	Solvent (1:1)	Base	Time (h)	Yield (%) ^b
1	0	H ₂ O	KOH	72	0
2	4	H ₂ O	KOH	30	78
3	5	H ₂ O	KOH	28	85
4	7	H ₂ O	KOH	24	95
5	10	H ₂ O	KOH	24	96
6	7	DMSO/H ₂ O	KOH	20	75
7	7	PEG	KOH	35	50
8	7	DMF	KOH	35	55
9	7	DMSO	KOH	35	57
10	7	H ₂ O	NaOH	28	80
11	7	H ₂ O	K ₂ CO ₃	40	<1
12	7	H ₂ O	K ₃ PO ₄	40	<1
13 ^c	7	H ₂ O	KOH	21	70

^a Reaction conditions: PhI (1.0 mmol), Base (2.0mmol),^b Isolated Yield. ^c Solution at 80 °C.

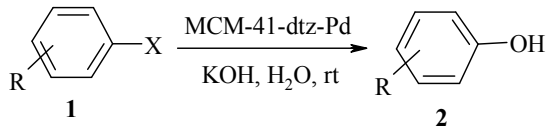
Table 2. Phenol formation vs symmetric diaryl ether formation



Entry	Base	Time (h)	phenol	Ether
1	KOH (2 mmol)	24	95%	5%
2	KOH (1 mmol)	28	80%	20%
3	K ₂ CO ₃ (2 mmol)	40	<1%	99%

The results of hydroxylation of various aryl halides have been summarized in Table 3.

Table 3. Synthesis of phenols from aryl halides in the presence of MCM-41-dtz-Pd



Entry	Aryl halide 1	Time (h)	Yield 2 (%) ^{a,b}	Mp (°C) [Ref.]
1		24	95	40 [48]
2		27	87	54-56[35]
3		24	84	35-36 [48]
4		28	88	40[48]
5		23	95	113-115 [33]
6		25	85	110-113 [33]
7		30	77	32-34 [48]
8		25	80	35-36 [48]
9		26	78	94-96 [33]
10		33	60	40 [48]
11		25	88	113-115 [33]
12		28	70	110-113 [33]
13		36	64	54-56[35]

^a All products were identified and characterized by comparison of their physical and spectral data with those of authentic samples. ^b Isolated yield.

After successful synthesis of a wide range of phenols in excellent yields, we explored the use of described catalytic system for the synthesis of aniline derivatives from aryl halides and $\text{NH}_3 \cdot \text{H}_2\text{O}$. The preliminary investigation was the screening of solvent, base and different amounts of catalyst on the outcome of the reaction of iodobenzene with $\text{NH}_3 \cdot \text{H}_2\text{O}$ (Table 4).

Table 4. Optimization of different parameters for the amination of iodobenzene with $\text{NH}_3 \cdot \text{H}_2\text{O}$ ^a

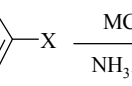
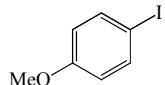
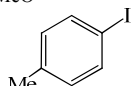
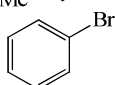
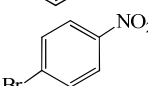
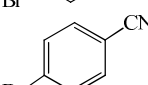
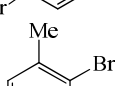
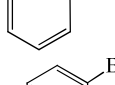
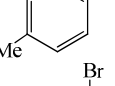
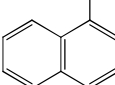
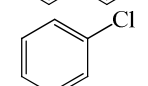
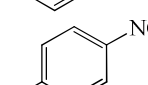
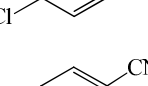
Entry	Cat. (mg)	Solvent	Base	Time (h)	Yield (%) ^b
1	0	H_2O	K_2CO_3	72	0
2	4	H_2O	K_2CO_3	15	80
3	5	H_2O	K_2CO_3	14	85
4	7	H_2O	K_2CO_3	12	93
5	10	H_2O	K_2CO_3	13	92
6	7	H_2O	KOH	14	70
7 ^c	7	H_2O	K_2CO_3	17	85
8 ^d	7	H_2O	K_2CO_3	20	70
9	7	DMSO/ H_2O	K_2CO_3	16	78
10	7	PEG	K_2CO_3	20	60
11	7	DMF	K_2CO_3	18	55
12	7	DMSO	K_2CO_3	19	60
13	7	H_2O	Et_3N	30	52
14	7	H_2O	$n\text{Pr}_3\text{N}$	30	45
15	7	DMSO/ H_2O	Et_3N	30	50
16 ^e	7	H_2O	K_2CO_3	10	90

^a Reaction conditions: PhI (1.0 mmol), Base (1.5 mmol),

^b Isolated yield. ^c $\text{NH}_3 \cdot \text{H}_2\text{O} = 8$ equiv. ^d $\text{NH}_3 \cdot \text{H}_2\text{O} = 5$ equiv. ^e Temperature = 80°C .

The model reaction was carried out in the presence of different solvents, bases and different amounts of reactants and catalyst. The best results were obtained with iodobenzene (1.0 mmol), $\text{NH}_3 \cdot \text{H}_2\text{O}$ (10 equiv.) and K_2CO_3 (1.5 mmol) in the presence catalytic amounts of MCM-41-dtz-Pd (7 mg) in H_2O as solvent at room temperature (Table 4, entry 4). After optimizing the reaction conditions, the coupling reaction of various aryl halides with $\text{NH}_3 \cdot \text{H}_2\text{O}$ has been performed. Results have been summarized in Table 5. As shown in Table 5, all of the examined aryl halides reacted with aqueous ammonia to afford the corresponding anilines with good to excellent yields. On the other hand, aryl halides bearing electron-donating substituents were less effective. In addition, the reactivity of aryl chlorides decreased dramatically in the present system.

Table 5. Preparation of aniline derivatives from aryl halides in the presence of catalytic amounts of MCM-41-dtz-Pd

Entry	Aryl halide 1	Time (h)	Yield 3 (%) ^{a,b}	Mp ($^\circ\text{C}$) [Ref.]
1		12	93	yellow oil [48]
2		15	88	56-59[26]
3		13	85	42-44 [48]
4		15	85	yellow oil [48]
5		11	95	146-149 [26]
6		13	88	83-85 [48]
7		18	72	yellow oil [48]
8		14	80	42-44 [48]
9		15	80	48-50 [48]
10		20	70	yellow oil [48]
11		15	75	146-149 [26]
12		17	63	83-85 [48]
13		23	60	56-59[26]

^a All of the products were identified and characterized by comparison of their physical and spectral data with those of authentic samples. ^b Isolated yield.

Finally, the reusability of the MCM-41-dtz-Pd was investigated. Fig. 6 shows the yield of five consecutive cycles for the preparation of phenol (a) and aniline (b) from iodobenzene. After the reaction completion, the catalyst was recovered, washed with ethanol and water, and then reused in the next run. The catalyst has been observed to be reusable for at least five times without a detectable catalytic leaching or an appreciable change in its activity (Fig. 6). High and reproducible catalytic activity and significantly low leaching of Pd (during catalytic reaction) from MCM-41 functionalised with dithizone (dtz) ligand was observed (only about 1%), the amount of Pd in the five recovery determined by EDS spectrum. Based on EDS measurement mas relative quantity of Pd has been determined for unreacted catalyst, which was 39.03% and after fifth run that was 33.89%. Also, the nature of the recovered catalyst was investigated by FT-IR (Fig. 7) and XRD pattern (Fig. 8). FT-IR and XRD pattern of recovered catalyst indicates that the catalyst can be recycled five times without any significant change in its structure or mesoporosity of silicate parent.

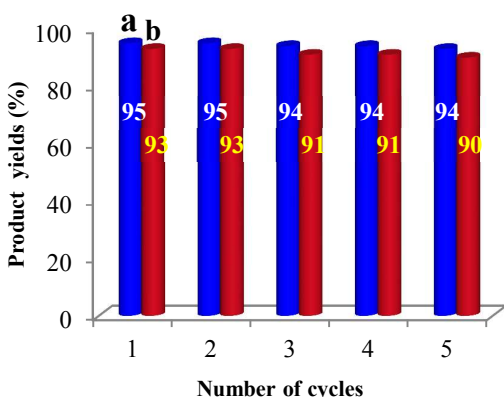


Figure 6. Reusability of MCM-41-dtz-Pd in the hydroxylation of iodobenzene (columns a) and the amination of iodobenzene with $\text{NH}_3 \cdot \text{H}_2\text{O}$ (columns b)

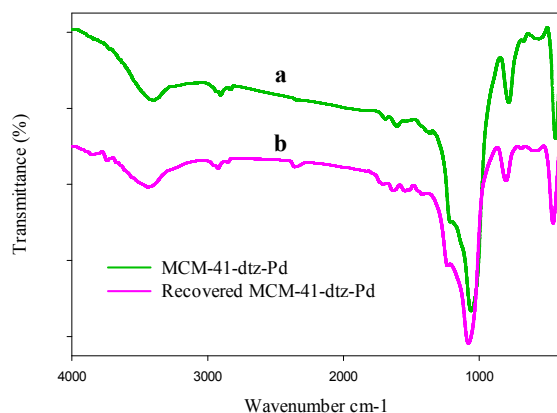


Figure 7. FT-IR spectra of (a) MCM-41-dtz-Pd (b) recovered MCM-41-dtz-Pd.

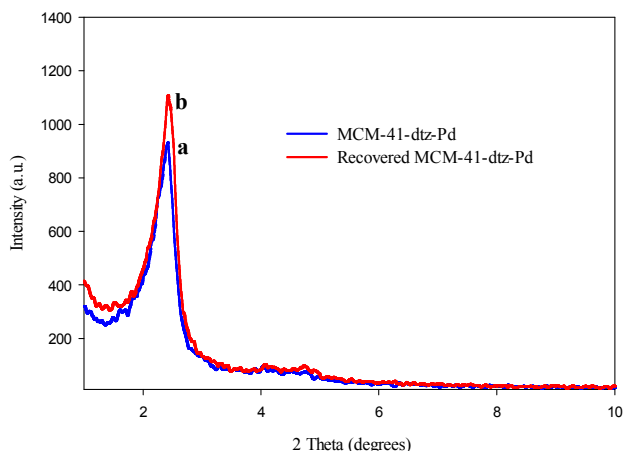


Figure 8. Low angle XRD patterns of (a) MCM-41-dtz-Pd and (b) recovered MCM-41-dtz-Pd.

3 Conclusions

In summary, we have developed a simple and efficient palladium-catalyzed method for the synthesis of phenol and aniline derivatives from aryl halides at “Room Temperature” in “Water”. A novel Pd complex supported on dithizone-functionalized nanostructured MCM-41 has been prepared through sequential grafting of several organic molecules under mild reaction conditions through Sol-gel synthesis. This study showed particle size of approximately 25 to 60 nm for the mesoporous catalyst. The catalyst has high thermal and chemical stability and is an efficient and recyclable catalyst for the reaction of a wide variety of aryl halides with KOH and $\text{NH}_3 \cdot \text{H}_2\text{O}$. The ease of preparation, long shelf life, simple separation from the reaction mixture, stability toward air and compatibility with a wide variety of coupling reactions make it an ideal green heterogeneous catalyst. Moreover, the catalyst could be reused for several cycles without significant loss of stability and activity. These advantages make the process valuable from the synthetic and environmental points of view.

4 Experimental

4.1. Material and physical measurements

The cationic surfactant cetyltrimethylammonium bromide (CTAB, 98%), tetraethyl orthosilicate (TEOS, 98%), sodium hydroxide, aryl halide and solvents were purchased from Merck and Aldrich chemical companies and used without further purification. Catalyst was characterized by XRD patterns, which were collected on a Scintag PAD V X-Ray diffractometer using a Co radiation source with a wavelength $\lambda = 1.78897 \text{ \AA}$, 40 kV. The particle morphology was examined by measuring SEM using FESEM-TESCAN MIRA3. TEM analysis of the catalyst was recorded using a Zeiss-EM10C TEM. IR spectra were recorded as KBr pellets on a VRTEX 70 model BRUKER FT-IR spectrophotometer. NMR spectra were recorded with a Bruker AVANCE DPX-300 (300 MHz for ^1H). Chemical shifts are given in ppm (δ)

relative to internal TMS and coupling constants J are reported in Hz. Mass spectra were recorded with an Agilent-5975C inert XL MSD mass spectrometer operating at an ionization potential of 70 eV. TGA was carried out on Shimadzu DTG-60 instrument. The content of Pd was measured by inductively coupled plasma-optical emission spectrometry (ICP-OES). Melting points were measured with an Electrothermal 9100 apparatus.

4.2 Preparation of mesoporous silica-anchored MCM-41-dtz-Pd

Mesoporous Si-MCM-41 was prepared through Sol-gel synthesis according to the literature method with slight variations [49]. The synthesis procedures of Si-MCM-41 were as follows: 3.5 mL of NaOH (2 M) solution was mixed with 480 mL of deionized water, then 1.0 g of cetyltrimethylammonium bromide (CTAB) was added to the solution with stirring and heating at 80 °C, when the solution became homogeneous, 5 mL of TEOS was dropped in slowly, giving rise to a white slurry, after 2 h stirring, the resulting product was filtered, washed with deionized water and dried at 70 °C followed by calcination at 550 °C for 5 h with rate of 2 °C min⁻¹ to remove the residual surfactants. This mesoporous material is designated as Si-MCM-41. Functionalization of MCM-41 was performed by refluxing 4.8 g of Si-MCM-41 with 5.0 g of 3-chloropropyltrimethoxysilane (CPTMS) in *n*-hexane (96 mL) under nitrogen atmosphere for 24 h. The resulting solid MCM-41-(CH₂)₃-Cl was filtered and washed with *n*-hexane for several times and dried under vacuum. Then, MCM-41-(CH₂)₃-Cl (3 g) and dithizone (7.0 mmol) were added to a 100 mL round-bottomed flask containing DMF (20 mL) equipped with a magnetic stirrer bar. The reaction mixture was stirred for 30 h at 100 °C, filtered, washed thoroughly with ethanol and dried in vacuum for 12 h. The MCM-41-dtz (3.0 g) was treated with ethanol (50 mL) for 30 min. An ethanolic solution of Pd(OAc)₂ (1.2 g) was added and the resulting mixture was refluxed for 15 h. The resulting black solid impregnated with the metal complex was filtered and washed with ethanol to obtain MCM-41-dtz-Pd.

4.3 General experimental procedures for *O*-arylation

4.3.1 Hydroxylation of iodobenzene catalyzed by MCM-41-dtz-Pd

The prepared catalyst (7 mg) was added to a mixture of iodobenzene (1.0 mmol), KOH (2.0 mmol) and H₂O (3.0 mL) at room temperature. The progress of the reaction was monitored by TLC. The reaction mixture was stirred for 24 h. After completion of the reaction, 10 ml of ethyl acetate and 2 ml of aq. HCl (6 M HCl) were added to reaction mixture. The mixture were stirred for 30 min, then filtered and washed with 5 mL of ethyl acetate. The catalyst was separated and washed with ethanol and water, vacuum dried and stored for subsequent runs. Gathered aqueous phases were extracted with ethyl acetate for three times. The organic layer was dried over MgSO₄ and then evaporated under reduced pressure. The crude residue was purified by column chromatography on silica gel using *n*-hexane/EtOAc (80/20), afforded the phenol

in good yield. Reaction product was characterized by IR, ¹H NMR and MS spectrometry.

Selected spectroscopy data

Phenol (Table 3, entries 1, 4 and 10): White solid, mp. 40 °C [48]. ¹H NMR (300 MHz, CDCl₃): δ (ppm) 7.23 (t, J = 8.4 Hz, 2H), 6.92 (t, J = 7.5 Hz, 1H), 6.82 (d, J = 7.5 Hz, 2H), 5.10 (s, 1H); EI-MS (70eV): m/z = 94 (M⁺).

4-Nitrophenol (Table 3, entries 5 and 11): Yellow solid, mp. 113-115 °C [33]. ¹H NMR (300 MHz, CDCl₃): δ (ppm) 8.17 (d, J = 9.0 Hz, 2H), 6.93 (d, J = 9.0 Hz, 2H), 6.11 (s, 1H); EI-MS (70eV): m/z = 139 (M⁺).

4-Methoxyphenol (Table 3, entries 2 and 13): white solid, mp. 54-56 °C [35]. ¹H NMR (300 MHz, CDCl₃): δ (ppm) 6.80-6.75 (m, 4H), 4.56 (brs, 1H), 3.76 (s, 3H); EI-MS (70eV): m/z = 124 (M⁺).

4.4 General experimental procedures for *N*-arylation

4.4.1 Amination of iodobenzene catalyzed by MCM-41-dtz-Pd

Iodobenzene (1.0 mmol) was added to a stirring mixture of catalyst (7 mg) in H₂O (2.0 mL). Then, NH₃·H₂O (10 equiv.) and K₂CO₃ (1.5 mmol) were added and stirred at room temperature. Monitoring of the reaction with TLC analysis shown the reaction was completed 12 h. After the completion of the reaction, 10 ml of ethyl acetate was added to reaction mixture, then filtered and washed with 5 mL of ethyl acetate. The catalyst was separated and washed with ethanol and water, vacuum dried and stored for subsequent runs. Gathered aqueous phases were extracted with ethyl acetate for three times. The organic layer was dried over MgSO₄ and then evaporated under reduced pressure. The crude residue was purified by column chromatography on silica gel using *n*-hexane/EtOAc (70/30), afforded the aniline in good yield. Reaction product was characterized by IR, ¹H NMR and MS spectrometry.

Selected spectroscopy data

Aniline (Table 5, entries 1, 4 and 10): Yellow oil [48]. ¹H NMR (300 MHz, CDCl₃): δ (ppm) 7.12 (t, J = 10.0 Hz, 2H), 6.73 (t, J = 10.0 Hz, 1H), 6.63 (d, J = 11.2 Hz, 2H), 3.53 (s, 2H); EI-MS (70eV): m/z = 93 (M⁺).

p-Toluidine (Table 5, entries 3 and 8): White solid, mp. 42-44 °C [48]. ¹H NMR (300 MHz, CDCl₃): δ (ppm) 7.00 (d, J = 8.1 Hz, 2H), 6.63 (d, J = 8.1 Hz, 2H), 3.41 (s, 2H), 2.26 (s, 3H); EI-MS (70eV): m/z = 107 (M⁺).

4-Nitroaniline (Table 5, entries 5 and 11): yellow solid, mp. 146-149 °C [26]. ¹H NMR (300 MHz, CDCl₃): δ (ppm) 8.07 (d, J = 9.0 Hz, 2H), 6.63 (d, J = 9.0 Hz, 2H), 4.37 (s, 2H); EI-MS (70eV): m/z = 138 (M⁺).

Acknowledgements

We are thankful to the University Of Kurdistan Research Council for partial support of this work.

References

- E. Rafiee and S. Eavani, *Green Chem.*, 2011, **13**, 2116.
- A. Modak, J. Mondal, M. Sasidharan and A. Bhaumik, *Green Chem.*, 2011, **13**, 1317.
- L. Guanghua, W. Mai, R. Jinand and L. Jao, *Synlett*, 2008, 1418.
- T. J. Yoon, W. Lee, Y. S. Oh and J. K. Lee, *New. J. Chem.*, 2003, **27**, 227.
- F. Dehghani, A. R. Sardarian and M. Esmaeilpour, *J. Organometal. Chem.*, 2013, **743**, 87.
- Y. Zhu, L. P. Stubbs, F. Ho, R. Liu, C. P. Ship, J. A. Maguire and N. S. Hosmane, *Chem. Cat. Chem.*, 2010, **2**, 365.
- S. Shylesh, V. Schunemann and W. R. Thiel, *Angew. Chem. Int. Ed.*, 2010, **49**, 3428.
- C. T. Kresge, M. E. Leonowicz, W. J. Roth, J. C. Vartuli and J. S. Beck, *Nature*, 1992, **359**, 710.
- F. Torney, B. G. Trewyn, V. S. Y. Lin and K. Wang, *Nature Nanotech.*, 2007, **2**, 295.
- M. Hajjami, F. Ghorbani and F. Bakhti, *Appl. Catal. A.*, 2014, **470**, 303.
- R. M. Martin-Arand and J. Cejka, *Top Catal.*, 2010, **53**, 141.
- S. L. Jain, B. S. Rana, B. Singh, A. K. Sinha, A. Bhaumik, M. Nandi and B. Sain, *Green Chem.*, 2010, **12**, 374.
- L. Lv, K. Wang and X. S. Zhao, *J. Colloid Interface Sci.*, 2007, **305**, 218.
- M. Yoshikazu, Y. Masanori, A. Eiichi, A. Sadao and T. Shunsuke, *Ind. Eng. Chem. Res.*, 2009, **48**, 938.
- I. I. Slowing, J. L. Vivero-Escoto, C. W. Wu and V. S. Y. Lin, *Adv. Drug Deliv. Rev.*, 2008, **60**, 1278.
- J. Y. Ying, C. P. Mehnert and M. S. Wong, *Ang. Chem. Int. Ed.*, 1999, **38**, 56.
- J. Demel, Sujandi, S-E. Park, J. Cejka and P. Stepnicka, *J. Mol. Catal. A: Chem.*, 2009, **302**, 28.
- J. Demel, M. Lamac, J. Cejka and P. Stepnicka, *Chem. Sus. Chem*, 2009, **2**, 442.
- B. Karimi, S. Abedi, J. H. Clark and V. Budarin, *Angew. Chem. Int. Ed.*, 2006, **45**, 4776.
- C. W. Cheung and S. L. Buchwald, *J. Org. Chem.*, 2014, **79**, 5351.
- M. K. Elmekdem, C. Fischmeister, C. M. Thomas and J. L. Renaud, *Chem. Commun.*, 2010, **46**, 925.
- J. H. P. Tyman, *Synthetic and Natural Phenols*; Elsevier: New York, 1996.
- S. Bräse, A. Encinas, J. Keck and C. F. Nising, *Chem. Rev.*, 2009, **109**, 3903.
- L. Jing, J. Wei, L. Zhou, Z. Huang, Z. Li and X. Zhou, *Chem. Commun.*, 2010, **46**, 4767.
- D. B. Zhao, N. J. Wu, S. Zhang, P. H. Xi, X. Y. Su, J. B. Lan and J. S. You, *Angew. Chem. Int. Ed.*, 2009, **48**, 8729.
- K. G. Thakur, K. S. Srinivas, K. Chiranjeevi and G. Sekar, *Green Chem.*, 2011, **13**, 2326.
- S. Enthaler and A. Company, *Chem. Soc. Rev.*, 2011, **40**, 4912.
- Y. Xiao, Y. Xu, H. S. Cheon and J. Chae, *J. Org. Chem.*, 2013, **78**, 5804.
- C. B. Lavery, N. L. RottaLoria, R. McDonald and M. Stradiotto, *Adv. Synth. Catal.*, 2013, **355**, 981.
- O. Songis, P. Boulens, C. G. M. Benson, and C. S. J. Cazin, *RSC Adv.*, 2012, **2**, 11675.
- A. Tlili, N. Xia, F. Monnier and M. Taillefer, *Angew. Chem. Int. Ed.*, 2009, **48**, 8725.
- D. Yang and H. Fu, *Chem. Eur. J.*, 2010, **16**, 2366.
- K. G. Thakur and G. Sekar, *Chem. Commun.*, 2011, **47**, 6692.
- K. Yang, Z. Li, Z. Wang, Z. Yao and S. Jiang, *Org. Lett.*, 2011, **13**, 4340.
- C. W. Yu, G. S. Chen, C. W. Huang and J. W. Chern, *Org. Lett.*, 2012, **14**, 3688.
- A. G. Sergeev, T. Schulz, C. Torborg, A. Spannenberg, H. Neumann and M. Beller, *Angew. Chem. Int. Ed.*, 2009, **48**, 7595.
- A. Dumrath, X. F. Wu, H. Neumann, A. Spannenberg, R. Jackstell and M. Beller, *Angew. Chem. Int. Ed.*, 2010, **49**, 8988.
- G. D. Vo and J. F. Hartwig, *J. Am. Chem. Soc.*, 2009, **131**, 11049.
- D. E. Bergbreiter, P. L. Osburn and J. D. Frels, *J. Am. Chem. Soc.*, 2001, **123**, 11105.
- J. M. Zhou, R. X. Zhou, L. Y. Mo, S. F. Zhao and X. M. Zheng, *J. Mol. Catal.*, 2002, **178**, 289.
- M. Opanasenko, P. Stepnicka and J. Cejka, *RSC Adv.*, 2014, **4**, 65137.
- A. Ghorbani-Choghamarani, F. Nikpour, F. Ghorbani and F. Havasi, *RSC Adv.*, 2015, **5**, 33212.
- M. Nikoorazm, A. Ghorbani-Choghamarani, H. Mahdavi and S. MostaffaEsmaeili, *Microporous and Mesoporous Materials*, 2015, **211**, 174.
- M. Nikoorazm, A. Ghorbani-Choghamarani, F. Ghorbani, H. Mahdavi and Z. Karamshahi, *J. Porous. Mater.*, 2015, **22**, 261.
- C. C. Torres, C. H. Campos, J. L. G. Fierro, P. Reyes and D. Ruiz, *J. Mol. Catal. A Chem.*, 2014, **392**, 321.
- M. Abrantes, A. Sakthivela, C. C. Romão and F. E. Kühn, *J. Organomet. Chem.* 2006, **691**, 3137.
- A. Benhamou, M. Baudu, Z. Derriche and J. P. Basly, *J. Hazard. Mater.*, 2009, **171**, 1001.
- H. J. Xu, Y. F. Liang, Z. Y. Cai, H. X. Qi, C. Y. Yang and Y. S. Feng, *J. Org. Chem.*, 2011, **76**, 2296.
- Q. Cai, Z. S. Luo, W. Q. Pang, Y. W. Fan, X. H. Chen and F. Z. Cui, *Chem. Mater.*, 2001, **13**, 258.